CONF-960536--3

A BLOOD CIRCULATION MODEL FOR REFERENCE MAN

R. W. Leggett[1], L. R. Williams[2], K. F. Eckerman[1]
[1]Dosimetry Research Group
Health Sciences Research Division
Oak Ridge National Laboratory
Oak Ridge, Tennessee 37831-6480
and
[2]Division of Liberal Arts and Sciences
Indiana University South Bend
South Bend, IN 46634

ABSTRACT

This paper describes a dynamic blood circulation model that predicts the movement and gradual dispersal of a bolus of material in the circulation after its intravascular injection into an adult human. The main purpose of the model is to improve the dosimetry of internally deposited radionuclides that decay in the circulation to a significant extent. The total blood volume is partitioned into the blood contents of 24 separate organs or tissues, right heart chambers, left heart chambers, pulmonary circulation, arterial outflow to the systemic tissues (aorta and large arteries), and venous return from the systemic tissues (large veins). As a compromise between physical reality and computational simplicity, the circulation of blood is viewed as a system of first-order transfers between blood pools, but outflow from any given pool is delayed during the first pass of material through the circulation with the delay time depending on the mean transit time across the pool. The model allows consideration of incomplete, tissue-dependent extraction of material during passage through the circulation and return of material from tissues to plasma.

INTRODUCTION

The International Commission on Radiological Protection (ICRP) currently is revising its document on Reference Man (1). As part of this revision, we have reviewed information on the human circulation and in previous papers and reports (2-4) have proposed reference values for total and regional blood volumes, cardiac output, and regional blood perfusion rates. In this paper we summarize the main features of a dynamic blood flow model that unifies the information described in the previous papers, and we illustrate how the model can be used to predict the

DISCLAIMER

distribution of decays of short-lived radionuclides after intravenous injection into an adult human. Details concerning model parameters and solution of the model can be found in Ref. 5.

The model is a compromise between physical reality and computational simplicity. The circulation of blood is viewed as a system of first-order transfers among 29 blood pools, together with a set of delays in transfer of material from one pool to the next. The delays are used only during the first pass after injection of material into blood, because use of subsequent delays would complicate the implementation of the model while making little difference in dosimetric estimates. For purposes of radiation dosimetry, the first-pass delays may be ignored for radionuclides with half-lives longer than about 3 min.

Transfer rates between compartments are derived from input values for total blood volume, total cardiac output, the fraction of the total blood volume contained in each compartment, and the fraction of cardiac output received by each compartment. A full set of input values has been derived only for the baseline case of a 35-y-old, resting adult male. In subsequent work we will extend input values to females and children and use the model to address the age- and gender-specific dosimetry of some medically important radionuclides.

MODEL STRUCTURE

A schematic diagram of the model is shown in Fig. 1. The total blood volume is partitioned into 29 compartments, including 24 compartments representing the nutrient blood supplies of organs or tissues and five compartments corresponding to venous return from the systemic tissues (large veins in Fig. 1), contents of right and left heart chambers, contents of the pulmonary circulation, and arterial outflow to the systemic tissues (aorta and large arteries in Fig. 1, sometimes referred to as the "large artery pool"). The 24 nutrient compartments include a pool called "all other" that represents the collective nutrient blood supply of organs and tissues not explicitly identified in Fig. 1, such as the eyes, pituitary gland, and salivary glands. As described later, an additional compartment called "injection vein" is used to address the delayed entry of intravenously injected material into the right heart.

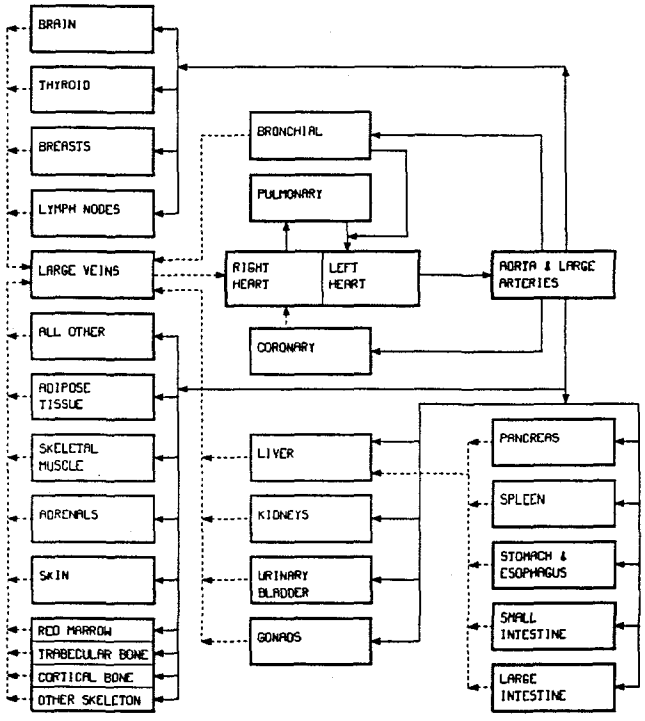

Figure 1. Diagram of the blood flow model.

The blood content of the heart is partitioned into right heart (right atrium plus right ventricle), left heart (left atrium plus left ventricle), and the coronary pool that supplies nutrients to the heart. Venous return from the systemic circulation flows into the right heart, is pumped via the pulmonary circulation through the lungs, enters the left heart, and then is pumped into the aorta. The coronary circulation is fed by the aorta. In reality, blood leaves the coronary circulation through a complicated system of vascular connections with the various cardiac chambers (6), but in this model the simplifying assumption is made that venous outflow from the coronary pool is received by the right heart.

The blood in the lungs is partitioned into a pulmonary pool that receives oxygen from the lungs and a bronchial pool that supplies nutrients to the lungs. The bronchial circulation is assumed to be fed by the aorta and to return blood to the systemic venous system (one-third of venous outflow) and the left heart (two-thirds of venous outflow). The model does not include some generally less important aspects of the bronchial circulation, such as shunting of bronchial arterial flow to the systemic circulation or various connections between the bronchial and the pulmonary circulations (6,7-10).

The portion of the cardiac output known as the portal circulation flows through capillary beds of the spleen, pancreas, stomach, intestines, and part of the esophagus, merges in the portal vein, and is then circulated through the liver. The stomach and esophagus are lumped because of their close relation in the body and because the limited amount of data on the esophagus suggest a blood perfusion rate similar to that of the stomach (11). Although venous outflow from much of the esophagus and from the anal canal do not pass through the liver, this "non-portal" flow typically represents a small portion of the total venous outflow from the alimentary tract and is not depicted in this model. The model also does not depict collateral circulation from the liver to the lungs, which may become important in some diseases (2).

The kidneys, urinary bladder, gonads, brain, thyroid, breasts, lymph nodes, adipose tissue, skeletal muscle, adrenals, skin, skeletal compartments, and all other (all remaining tissues combined into a single compartment) are assumed to be fed only by the large arteries, and venous outflow is assumed to be only to the large veins. The breasts are included as a separate compartment for application of the model to mature or adolescent females. The complex blood supply of the skeleton (12) is simplified considerably by viewing the four skeletal compartments as parallel blood pools (Fig. 1).

The model may be thought of as describing the flow of blood or some component of blood such as blood plasma or red blood cells, or the movement of an internally deposited substance as it is carried in blood. The simplifying assumption is made that all components of blood have the same kinetics. This assumption is not strictly true. For example, it is known that red blood cells and plasma have different rates of transfer through some vascular beds (13,14). However, there is insufficient information to model the differential kinetics of different blood components with much confidence.

For the case of intravenous injection of a substance, the injected material is depicted as passing in series through the injection vein, the right heart chambers, the pulmonary pool, the left heart chambers, and the aorta and large arteries, with brief delays in each pool before outflow to the next pool begins. Outflow from the large artery pool is assumed to be distributed among the vascular beds of the different tissue compartments according to the distribution of cardiac output. After compartment-specific delays in the blood and tissue pools of each of the tissue compartments, material begins to flow out of the different compartments into the large veins.

After a brief delay, material in the large veins reaches the right heart and begins a new cycle through the circulation. As described below, no further delays are imposed after the first pass through the circulation.

DERIVATION OF TRANSFER RATES AND DELAYS FOR THE REFERENCE ADULT MALE

Baseline Parameter Values

The kinetics of blood circulation is complex but for most practical purposes can be viewed as a system of first-order transfers among the different blood pools, together with a set of delays, or minimal transit times, in transfer of material from one pool to the next. These delays are used only during the first pass after injection of material into blood, because depiction of subsequent delays would complicate the implementation of the model and would make little difference in predictions of the distribution of the material.

The first-order transfer rates between compartments and the delays imposed during the first pass are all secondary values that are derived from the following input parameters: the total blood volume (ml); the cardiac output (ml d^{-1}); 29 regional blood volumes (i.e., the fraction of the total blood volume contained in each of the 29 compartments shown in Fig. 1); 24 fractional blood flows to compartments fed by aorta and large arteries; and, for the case of intravenous injection of material, a delay period in the injection vein representing the time between the start of injection and the beginning of inflow into the right heart, and a transfer rate from the injection vein into the right heart.

Baseline values for total blood volume and cardiac output in a healthy, reclining, 35-y-old male are 5300 ml and 6500 ml min^{-1}, respectively (4). Baseline values for regional blood volumes and the distribution of cardiac output in a healthy, reclining, 35-y-old male are given in Table 1. These reference values are based on the authors' review and reanalysis of data from about 500 studies of blood flow and blood volume in human subjects and laboratory animals. Data reduction and selection of reference values, as well as the potential variability of blood volume and flow with such factors as sex, age, and level of activity, are described elsewhere (2-4). Additional information on the division of skeletal blood flow among red marrow, trabecular bone, cortical bone, and other skeletal tissues was found in Refs. 12 and 15-19. Reference values for blood volume and blood flow of the four skeletal compartments are more reflective of the relative sizes of nutrient blood supplies of these compartments than of their total internal vasculature; this approach was judged to be appropriate for purposes of radiation dosimetry.

Delays in transfer between blood pools during the first pass

If a radioactive tracer is injected into an arm vein, say, of an adult male at time 0, activity could reach the pulmonary circulation in as little as 5-6 s, some systemic tissues in 11-12 s, and venous outflow from some tissues in 15 s (Table 2). The initial appearance time (AT) of the tracer in the right heart, lung, or large arteries is noticeably smaller than the mean transit time (MTT) of the tracer to these points. Even smaller ratios of AT:MTT have been determined for transit across the nutrient beds of organs and tissues. Reported measurements of AT and MTT for various injection and measurement sites in the circulation indicate a ratio AT:MTT in the range 0.6-0.85 for flow through portions of the central circulation and a median ratio near 0.5 for flow across a nutritive vascular bed (5).

Table 1. Reference regional blood volumes and flow rates for organs of a recumbent adult male

Organ or tissue	% of total blood volume	% cardiac output received
adipose tissue	5.0 (4-8)	5.0 (3.5-9)
brain	1.2 (0.8-1.4)	12.0 (10-15)
stomach and esophagus	1.0 (0.2-1.3)	1.0 (0.5-2)
small intestine	3.8 (0.9-4.4)	10.0 (7-13)
large intestine	2.2 (0.5-2.5)	4.0 (2.8-6)
heart		
chambers	9.0 (6-12)	
coronary tissue	1.0 (0.5-1.5)	4.0 (3-6)
kidneys	2.0 (1.3-2.9)	19.0 (16-21)
liver	10.0 (4-12)	6.5 (5.5-8.5) arterial 25.5 (17-30) total
pulmonary	10.5 (8-13)	
bronchial tissue	2.0 (1.8-2.5)	2.5 (1-5.5)
skeletal muscle	14.0 (8-21)	17.0 (10-21)
pancreas	0.6 (0.1-0.7)	1.0 (0.6-1.9)
skeleton	7.0 (4-8) total	5.0 (2.5-10) total
red marrow	4.0	3.0
trabecular bone	1.2	0.9
cortical bone	0.8	0.6
other skeleton	1.0	0.5
skin	3.0 (1-6)	5.0 (3.3-7)
spleen	1.4 (1.2-1.9)	3.0 (2.5-5)
thyroid	0.06 (0.02-0.1)	1.5 (0.7-2.2)
lymph nodes	0.2 (0.05-0.4)	1.7 (0.5-3.5)
testes	0.04 (0.01-0.1)	0.05 (0.01-0.1)
adrenals	0.06 (0.01-0.1)	0.3 (0.1-1)
urinary bladder	0.02 (0.01-0.05)	0.06 (0.01-0.2)
all other tissues	1.92 (1-4)	1.39 (0.5-3.5)
aorta and large arteries	6.0 (3-9)	
large veins	18.0 (11-25)	

Table 2. Comparison of experimentally determined circulation times with model predictions; based on Table 2 of Ref. 5, where original studies are cited

Path	Appearance time (s)		Mean transit time (s)	
	Observed	Model	Observed	Model
Right heart to left heart	5	5.2	6.5	7.5
Right heart to aorta			8	9.7
Right heart to radial artery	9.5	8.4		
Arm vein to pulmonary artery			6.5	7.9
Pulmonary artery to radial artery	9	6.8	12	9.6
Pulmonary artery to tongue	7	7.3		
Arm vein to femoral artery	12	12	18	18
Basilic vein to brachial artery			19	17
Brachial vein to brachial artery	5	8.8	14	12
Arm vein to brain	12	13	18	18
Brachial vein to jugular vein	9	13	17	19
Antecubital vein to hepatic vein	27	22		
Liver to hepatic vein	10	9.7		
Superior mesenteric artery to spleen	4	11	19	23
Sup. mesenteric artery to portal vein	8.5	9.3		
Sup. mesenteric vein to sup. mes. artery	19	18		
Jugular vein to jugular artery			22	17
Carotid artery to jugular vein	3	3.5	7	6.3

To model the delay between injection of material into blood and the initial appearance of material at different points in the circulation, we assign to each blood pool a delay between the appearance time of material in the pool and the time material begins to flow out of the pool. The delay times for the different blood pools are related to the mean transit times across the pools. For right heart, left heart, pulmonary blood, aorta and large arteries, and large veins, the delay is assumed to be 0.7 times the mean transit time across the pool. For each nutrient blood pool, the

delay is assumed to be 0.5 times the mean transit time across the organ. For a given pool, the delay period begins when material first reaches the pool and applies only to the first pass of material through the pool; after the end of the delay period, outflow from the pool is assumed to follow first-order kinetics. The simple first-pass delay scheme used in this model is likely to overestimate the actual transit times of small portions of material through short circuits of some organs and tissues, but such overestimates will be of little practical consequence with regard to radiation dosimetry.

The mean transit time for a given pool is calculated as the volume of blood in the pool divided by the rate of flow of blood into the pool. For example, the brain is assumed to contain 1.2% of the total blood and to receive 12% of the cardiac outflow (Table 1). Based on a total-body blood volume of 5300 ml and cardiac output of 6500 ml min^{-1}, the mean transit time across the brain (i.e., from arterial inflow to venous outflow) is calculated as (0.012 × 5300 ml)/(0.12 × 6500 ml min^{-1}) = 4.89 s. For a material injected into blood, the delay between the first appearance in the brain circulation and the first appearance in venous outflow is assumed to be 0.5 × 4.89 s = 2.45 s. As a second example, the aorta and large arteries receive virtually 100% of the cardiac output and are assumed to contain 6% of the total blood (Table 1). Therefore, the mean transit time between entry of material into the aorta and exit into the systemic tissues is calculated as (0.06 × 5300 ml)/(1.0 × 6500 ml min^{-1}) = 2.94 s. After injection of a substance into blood, the delay between the first appearance in the aorta and large arteries and the beginning of exit from this pool (i.e., the first appearance in systemic organs) is assumed to be 0.7 × 2.94 s = 2.05 s.

The default value for the delay time in the injection vein (i.e., appearance time in the right heart) for the reference adult male is 4 s. This value is based on observations of Kuikka and coworkers (20-21) for material injected into the antecubital (mid-arm) vein of resting subjects. When cardiac output is elevated above the resting level, a shorter delay time may be appropriate. The default delay for intra-arterial injection is 2 s, which is about the same as the delay for aorta and large arteries.

The model may be applied to a continuous infusion as well as to acute injection of material into blood. The first-pass delays of continuously infused material can be accounted for by first generating a time-dependent activity curve for each compartment based on acute injection into the appropriate blood compartment and then convoluting the organ activity curves against the continuous infusion rate.

First-order transfer rates between blood pools

After the delay time is exceeded during the first pass of material through a given pool, outflow from the pool is assumed to follow first-order kinetics. The total transfer rate from a given pool to the receiving compartment(s) is calculated as the number of total blood volumes flowing into the pool per day, divided by the fraction of the total blood volume contained in the pool.

For example, the large veins are assumed to collect all of the venous outflow and hence all of the cardiac output, except that the coronary outflow is assigned to the right heart and two-thirds of the bronchial outflow is assigned to the left heart. Since the coronary pool receives 4% and the bronchial pool 2.5% of cardiac output, the large veins receive 100% - 4% -(2/3 × 2.5%) = 94.333% of cardiac output. The cardiac output is 1440 min d^{-1} × 6500 ml min^{-1} / 5300 ml = 1766 d^{-1}. Since the large veins are assumed to contain 18% of the total blood volume, the transfer rate from large veins to the right heart is calculated as 0.94333 × 1766 / 0.18 = 9255 d^{-1}.

The transfer rate (volumes d^{-1}) from the large artery pool into the blood pool of a systemic organ is calculated as $F_O \times CO / F_A$, where F_O = the fraction of cardiac output received by the organ, CO is the cardiac output (d^{-1}), and F_A is the fraction of the blood volume of the large artery pool. For example, the transfer rate from aorta and large arteries to coronary circulation is $0.04 \times 1766\ d^{-1} / 0.06 = 1177\ d^{-1}$.

The transfer rate from the blood pool of a systemic organ into the compartment designated as large veins (or into the liver via the portal vein) is calculated as the daily inflow into the pool, divided by the amount of blood in the pool. For example, the transfer rate from the kidney blood pool to large veins is calculated as $0.19 \times 1766\ d^{-1} / 0.02 = 16{,}777\ d^{-1}$.

Venous outflow from the spleen, pancreas, and alimentary tract is assumed to flow into the portal vein, which feeds the liver. The portal vein is not depicted explicitly in this model; rather, outflow from the pancreas, spleen, and alimentary tract is assigned directly to the liver blood pool. Outflow from the liver blood pool is assigned to the large veins.

The default transfer rate from injection vein to right heart in the reference resting adult male is 1/D, where D is the duration of injection. A transfer rate greater than (1/D) may be appropriate when cardiac output is elevated above the resting level.

Application of model to substances that transfer between blood and tissues

As illustrated later, the blood flow model may be used as a framework for modeling the kinetics of a substance that transfers between blood and extravascular pools. This requires the addition of extravascular compartments and derivation of substance-specific transfer rates between the blood compartments and extravascular compartments. Essentially, each of the organs fed by the large arteries (Fig. 1) is viewed as consisting of a blood compartment and one or more tissue compartments. In general, each tissue compartment may be treated as a peripheral compartment that exchanges material only with the blood compartment of the same organ. Transfer rates from one blood compartment to another are the same as described above for the blood flow model, and transfer rates between tissue compartments and blood are substance-specific.

The number of tissue compartments assigned to an organ will vary with the substance and/or the available biokinetic information. For short-lived radionuclides, it will often suffice to treat each organ as a single, well-mixed pool, because only short-term transfer from tissue to blood is of interest.

Depending on the type of biokinetic data available for a given substance, it may be possible to simplify the derivation of transfer rates to tissue compartments by treating the tissue and blood compartments of an organ as parallel rather than serial compartments. That is, one may assume that the tissue and blood compartments of an organ are both fed directly by the large artery pool (and portal vein, in the case of the liver) and that both lose material directly to the large vein pool. Such a scheme is physically incorrect but does not introduce significant temporal errors and has the advantage of allowing direct application of reported "extraction fractions" for substances. An extraction fraction for a given organ and a given substance in plasma (and for a given physiological condition) is the fraction of material removed by the organ during a single pass from arterial to venous plasma.

If the extraction fraction for a given substance and organ is known, then the transfer rates from the large artery pool to the organ blood pool and the organ tissue pool can be determined from that extraction fraction and the transfer rates of the basic blood flow model. For example,

the extraction fraction for Rb by brain appears to be on the order of 0.01. Since the brain is assumed to receive 12% of cardiac output, the transfer rate of blood from the large artery pool to the brain blood pool is $0.12 \times 1766\ d^{-1} / 0.06 = 3532\ d^{-1}$. With the parallel-compartment configuration, the transfer rate of Rb from the large artery pool to the brain blood pool would be $0.99 \times 3532\ d^{-1} = 3497\ d^{-1}$ and from the large artery pool to brain tissue would be $0.01 \times 3532\ d^{-1} = 35.32\ d^{-1}$.

COMPARISON OF MODEL PREDICTIONS WITH OBSERVATIONS OF THE EARLY KINETICS OF RADIO-TRACERS

Model predictions of transit times between different points in the circulation of a reference adult male are compared in Table 2 with observed values, i.e., central reported values for reasonably healthy adult humans, mainly males less than 50 years old. A model prediction for a given path, "Pool A to Pool B", refers to a travel time between the point of entry into Pool A and the point of entry into Pool B. To account for travel time between injection or sampling points and the receiving or feeding organs, the following appearance times are assumed: antecubital vein or median basilic vein to right heart, 4 s; brachial vein or jugular vein to right heart, 2 s; left heart to brachial artery or superior mesenteric artery, 1 s; left heart (exit) to radial or femoral artery, 2 s; brain (exit) to jugular vein, 0.5 s; carotid artery to brain, 0.5 s. For each of these portions of the "large veins" or "aorta and large artery" pools, the mean transit time is assumed to be 1.4 times the appearance time. For purposes of this exercise, "aorta" is interpreted as the point of entry into the "aorta and large artery" pool.

In Fig. 2, model predictions are compared with observations (22) of the concentration of ^{131}I in arterial and venous blood as a function of time after intravenous injection of ^{131}I-labeled human serum albumin into a resting adult human subject. The age, gender, or other characteristics of the subject were not reported. The observations in Fig. 2 represent radioactivity in blood samples collected over 15- or 30-s intervals from the brachial artery and hepatic vein. For purposes of this exercise the aorta and large artery pool of the model was used as a surrogate for brachial artery blood. A hepatic vein pool was created by separating venous outflow from the liver from all other flow into the large vein pool. The model curves in Fig. 2 are moving averages of predicted ^{131}I concentrations in these arterial and hepatic vein pools over 15-s intervals. All observations and model predictions were normalized to an arbitrary number (0.5) representing the concentration of ^{131}I in blood after a uniform distribution is attained. The model predictions were based on parameter values for the reference resting adult male. The default value of 4 s was used as the delay period in the injection vein, and the transfer rate from injection vein into right heart after the delay was assumed to be $0.5\ s^{-1}$ (rapid injection).

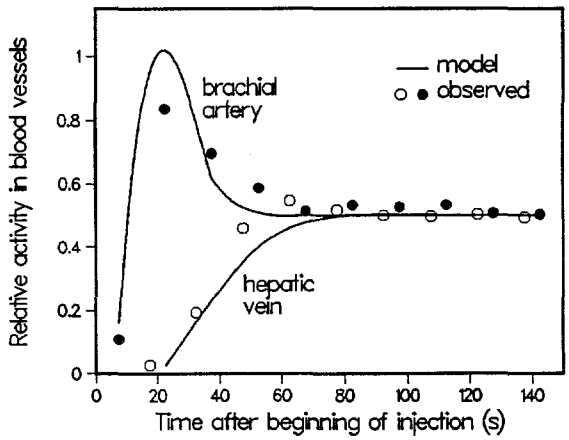

Figure 2. Observations and model predictions of radioactivity in arterial and venous blood of a subject after intravenous injection of ^{131}I-labeled human serum albumin.

APPLICATIONS AND DISCUSSION

Application to a radio-tracer that remains in blood

We consider the distribution of systemic decays of ^{11}C after inhalation of the tracer ^{11}C-labeled carbon monoxide (CO), which is rapidly absorbed to blood. Because absorbed CO is virtually completely bound to hemoglobin, it is reasonable to assume that all systemic decays of ^{11}C ($T_{1/2}$ = 20.4 min) occur in blood (23). In ICRP Publication 53 (23), this tracer is assumed to be distributed among tissues according to their blood contents at all times after absorption from the lungs to blood. With the present model, activity entering blood in the pulmonary compartment is viewed as passing in series through the pulmonary compartment, the left heart chambers, and the aorta and large arteries, and then distributing among the vascular beds of the different tissue compartments according to the distribution of cardiac output, which differs considerably from the distribution of blood volume.

To simplify comparison of predictions of the present blood flow model with those of the blood model of ICRP Publication 53, attention is confined to the integrated activity in the various blood pools, and the assumption is made that inhaled activity is instantaneously absorbed to blood. Predictions of the blood volume model of ICRP Publication 53 (23) were derived from fractional blood volumes given in Table A.2, p. 16, of that document.

Since ^{11}C has a relatively long half-life compared with the time required for activity in blood to become reasonably uniformly distributed (< 2 min), differences between predictions of the present model and that of ICRP Publication 53 (Table 3) arise mainly from differences in assumptions concerning regional blood volumes. The present model generates a considerably more detailed distribution of activity than does the model of ICRP Publication 53, which addresses only a small number of blood pools.

The model predictions for ^{11}C given in Table 3 are based on the baseline parameter values described earlier and hence do not consider differences between the distributions of red blood cells and plasma in the circulation. Such differences are conceivably important for ^{11}CO because of its rapid and nearly complete binding to red blood cells but were not addressed here due to a paucity of information for most of the compartments in this model.

Application to an ultrashort-lived radionuclide that transfers to extravascular spaces

The blood flow model is next used to predict the distribution of decays of intravenously injected ^{82}Rb, an ultrashort-lived radionuclide ($T_{1/2}$ = 75 s) used clinically in imaging of the myocardium, brain, and kidneys. Because Rb transfers rapidly from blood plasma to extravascular spaces, it is necessary to append extravascular compartments to the blood flow model and derive rates of transfer of Rb into these compartments. For each of the blood compartments fed by the large artery compartment, a corresponding tissue compartment is added to the model. We use the "parallel compartment" approach described in an earlier section and define transfer rates to these compartments in terms of Rb extraction fractions. Because of the short half-life of ^{82}Rb, we may assume that there is no transfer from tissues back to blood provided the applied extraction fractions are effective values over a few minutes rather than "first-pass" values. First-pass values sometimes overstate effective or steady-state extraction due to a brief delay in the onset of back diffusion of material from extravascular spaces to plasma.

Table 3. Comparisons of predicted cumulative activities in selected organs, based on the present blood flow model and the blood model of ICRP Publication 53 (23) for two cases: inhalation of ^{11}C-labeled carbon monoxide, and intravenous injection of ^{82}Rb

Organ or tissue	Ratio, ICRP Pub. 53 to this model	
	^{11}CO	^{82}Rb
adrenals	1.0	6.2
bone, cortical	2.7	7.8
bone, trabecular	0.4	1.3
red marrow	0.9	2.0
heart wall	1.3	1.6
kidneys	0.7	2.0
liver	0.5	0.9
lungs, pulmonary	0.8[a]	1.3
lungs, bronchial	--	0.2
pancreas	b	1.6
skeletal muscle	b	1.0
spleen	1.2	1.1
stomach and esophagus	b	2.1
small intestine	b	1.0
large intestine	b	1.4
thyroid	1.1	3.8

[a]Total lungs (pulmonary plus bronchial blood).
[b]Not included in blood volume model of ICRP Pub. 53.

In an earlier paper (24), biokinetic data on Rb were reviewed and a detailed biokinetic model for Rb was developed. That model included most of the tissue compartments indicated in Fig. 1 and made use of Rb extraction fractions but depicted plasma as a static, uniformly mixed pool that exchanged Rb with peripheral organs. The Rb extraction fractions derived in that paper are applied here to ^{82}Rb, except that extraction fractions for skeletal muscle and kidneys have been modified to accommodate differences in model structure and, in the case of kidneys, to reflect newer experimental data (25). The following extraction fractions are applied here: gastrointestinal tract compartments, lung, spleen, pancreas, skin = 0.80; skeletal muscle = 0.6; heart = 0.45; liver, skeleton = 0.4; brain = 0.01; and all other organs = 0.5.

These extraction fractions may be used, together with the transfer rates between blood pools described earlier, to derive transfer rates for this extension of the blood flow model to Rb. That is, each organ fed by aorta and large arteries is partitioned into a blood pool and a tissue pool. As illustrated in an earlier section, the transfer rate from aorta and large arteries to the tissue pool of a given organ is set at $E \times T$ and from aorta and large arteries to the blood pool of that organ is $(1 - E) \times T$, where E is the extraction fraction for the organ and T is the transfer rate from the aorta and large artery compartment to the organ. For each tissue pool, the transfer rate to the large veins (or liver) is set at zero; i.e., there is assumed to be no loss of ^{82}Rb from tissues. Transfers to or from heart chambers remain unchanged. Movement of ^{82}Rb along excretion pathways and uptake by red blood cells do not significantly influence the systemic distribution of decays of this ultrashort-lived radionuclide (24) and are not considered in the present calculations.

Integrated activity in the various organs as predicted by this extended blood flow model are compared in Table 3 with estimates from ICRP Publication 53 (p. 161 of Ref. 23). The assumed delay in the injection vein was 4 s. The transfer rate from injection vein to right heart was set at 1/5 s^{-1} for comparison of model predictions with ^{82}Rb-injection data of Ryan and coworkers (26), whose injection and subsequent saline flush were completed in 5-6 s. The estimate of the present model for an organ is the sum of activities in the blood pool and tissue pool of that organ. In ICRP Publication 53, the distribution of decays of ^{82}Rb is based on a model of the distribution of cardiac output. For example, 23% of the systemic decays were assigned to kidneys based on the assumption that the kidneys receive 23% of cardiac output. The delay time in the injection vein and the transfer rate to right heart assumed above do not apply to the model of ICRP Publication 53, because the residence time or location of activity in blood is not considered in that model. As indicated in Table 3, the method of ICRP Publication 53 yields higher estimates of integrated activity in most organs than does the present method. The differences in estimates result from two factors: the present method considers decays of ^{82}Rb that occur in blood pools outside the indicated organs; and the two different blood flow models underlying the two approaches depict considerably different blood flow rates to some pools (e.g., bronchial tissue and adrenals). For some of the listed organs, estimates of integrated activity cannot be derived from the blood flow model of ICRP Publication 53 (e.g., testes, urinary bladder).

Ryan and coworkers (26) used external measurements to estimate the integrated activity of intravenously injected ^{82}Rb in organs of two healthy men, ages 23 y and 27 y. For organs that could be reasonably well isolated by the external counting technique (liver, kidneys, and testes), model predictions were within 2-33% of experimentally determined values.

In Table 4 we compare estimates of absorbed dose from intravenously injected ^{82}Rb based on the present model as applied here to Rb (Method A) with absorbed dose estimates derived from five other models or methods for describing cumulative activities of ^{82}Rb (Methods B-F). Method B is a simplified version of our earlier Rb model (24), where compartments are assumed to receive ^{82}Rb in parallel from a single, central blood compartment in which injected ^{82}Rb is instantaneously mixed. Method C is the blood volume model of ICRP Publication 53 (23) as applied in that document to ^{82}Rb. Method D is based on the experimentally determined values of Ryan and coworkers (26) described above, using the average of cumulative activities for two subjects and assuming uniform distribution of activity in tissues not measured by Ryan and coworkers. Method E is based on cumulative activities of ^{86}Rb in rats at 1-180 min after injection and the assumption that individual organ concentrations per initial mean whole-body

Table 4. Comparison of absorbed dose estimates for intravenously injected ^{82}Rb in the adult male based on different models or methods

Organ or tissue	This model (Gy Bq^{-1} x 10^{12})	ICRP Pub. 53 (23) / This model	Ryan et al. (26)/ This model	Kearfott (27)/ This model	Uniform distribution/ This model
adrenals	3.6	5.9	0.1	0.2	0.1
red marrow	0.6	1.7	0.7	0.8	0.8
kidneys	9.2	2.0	1.0	0.6	0.05
liver	1.0	1.0	1.0	0.7	0.5
lungs	2.5	1.0	0.7	0.8	0.2
testes	0.3	0.4	0.8	0.4	1.3
thyroid	10	3.8	0.05	0.05	0.05

concentration are the same for humans and rats (27); as with Method D, activity not accounted for by measured pools was assumed to be uniformly distributed in the remainder of the body. Method F is the assumption of uniform distribution of activity in the body at all times after injection, which is equivalent to applying the Rb kinetic model of ICRP Publication 30 (28).

All absorbed dose estimates in Table 4 were based on specific effective energies and dosimetric methods described in a recent document by Cristy and Eckerman (29). Absorbed dose estimates based on Methods C, D, and E were generally close but not identical to estimates given in the original documents describing those methods (respectively, Refs. 23, 26, 27). Discrepancies appear to be due mainly to differences in the specific effective energies applied to total-body activity not contained in separately identified source organs, that is, activity in "other" or "remainder".

ACKNOWLEDGMENT

The work described in this paper was sponsored by the Office of Health and Environmental Research, U. S. Department of Energy, under contract DE-AC05-84OR21400 with Martin Marietta Energy Systems, Inc.

REFERENCES

1. International Commission on Radiological Protection (ICRP). Report of the task group on reference man. ICRP Publication 23. Pergamon Press, Oxford, 1975.

2. Williams LR, Leggett RW. Reference values for resting blood flow to organs of man. Clin Phys Physiol Meas 10:187-217, 1989.

3. Leggett RW, Williams LR. Suggested reference values for regional blood volumes in humans. Health Phys 60:139-154, 1991.

4. Williams LR. Reference values for total blood volume and cardiac output in humans. ORNL/TM-12814, Oak Ridge National Laboratory, Oak Ridge, TN, 1994.

5. Leggett RW, Williams LR. A proposed blood circulation model for Reference Man. Health Phys 69:187-201, 1995.

6. Brobeck JR. Best and Taylor's physiological basis of medical practice. Tenth edition. Williams and Wilkins, Baltimore, 1979.

7. Aramendia P, Martinez de Letona J, Aviado DM. Responses of the bronchial veins in a heart-lung bronchial preparation. Circ Res 10:3-10, 1962.

8. Aramendia P, Martinez de Letona J, Aviado DM. Exchange of blood between pulmonary and systemic circulations via bronchopulmonary anastomoses. Circ Res 11:870-879, 1962.

9. Aviado DM. The lung circulation. Vol. I, Physiology and pharmacology. Pergamon Press, New York, 1965.

10. Cudkowicz L. The human bronchial circulation in health and disease. Williams and Wilkins, Baltimore, 1968.

11. Pennanen MF, Bass BL, Dziki AJ, Harmon JW. Adenosine: differential effect on blood flow to subregions of the upper gastrointestinal tract. J Surg Res 56:461-465, 1994.

12. Kelly PJ. Pathways of transport in bone. In: Handbook of physiology, section 2: The cardiovascular system, vol. III, peripheral circulation and organ blood flow. Shepherd JT, Abboud FM, eds. pp. 371-396, American Physiological Society, Bethesda, MD, 1983.

13. Larsen OA, Tygstrup N, Winkler K. The splanchnic hematocrit in man. Acta Physiol Scand 57:397-406, 1963.

14. Ladefoged J, Pedersen F. Renal blood flow, circulation times and vascular volume in normal man measured by the intra-arterial injection -- external counting technique. Acta Physiol Scand 69:220-229, 1967.

15. Whiteside LA, Simmons DJ, Lesker P A. Comparison of regional bone blood flow in areas with differing osteoblastic activity in the rabbit tibia. Clin Orthop Rel Res 124:267-270, 1977.

16. Morris MA, Kelly PJ. Use of tracer microspheres to measure bone blood flow in conscious dogs. Calcif Tissue Int 32:69-76, 1980.

17. Gross PM, Marcus ML, Heistad DD. Current concepts review: measurement of blood flow to

bone and marrow in experimental animals by means of microsphere technique. J Bone Jt Surg 63-A:1028-1031, 1981.

18. Light TR, McKinstry MP, Schnitzer J, Ogden JA. Bone blood flow: regional variation with skeletal maturation. In: Bone circulation, Arlet J, Ficat RP, Hungerford DS (eds.), pp. 178-185, Williams and Wilkins, Baltimore, 1984.

19. Tøndevold E, Bülow J. Microsphere determined regional bone blood flow in conscious dogs at rest and long time muscular exercise. In: Bone circulation, Arlet J, Ficat RP, Hungerford DS (eds), pp. 175-177, Williams and Wilkins, Baltimore, 1984.

20. Kuikka JT, Pyorala T, Lehtovirta P, Rekonen A. Cardiopulmonary blood volumes at rest and during muscular exercise measured by ^{113m}In radiocardiography. Acta Physiol Scand 95, 145-152, 1975.

21. Kuikka J, Ahonen A. A simple and rapid non-invasive radioisotope method to determine ventricular ejection fractions and cardiopulmonary transit times. Nucl-Med Band XVI/Heft 2:57-62, 1977.

22. Bradley SE., Marks PA., Reynell PC, Meltzer J. The circulating splanchnic blood volume in dog and man. Transactions of the Association of American Physicians 66:294-302, 1953.

23. International Commission on Radiological Protection (ICRP). Radiation Dose to Patients from Radiopharmaceuticals. ICRP Publication 53. Pergamon Press, Oxford, 1987.

24. Leggett RW, Williams LR. A biokinetic model for Rb in humans. Health Phys 55: 685-702, 1988.

25. Mullani NA, Ekas RD, Marani S, Kim EE, Gould RL. Feasibility of measuring first pass extraction and flow with rubidium-82 in the kidneys. Amer J Physiologic Imaging 5:133-140, 1990.

26. Ryan JW, Harper PV, Stark VS, Peterson EL, Lathrop KA. Radiation absorbed dose estimate for rubidium-82 determined from in vivo measurements in human subjects. In: 4th Int. Radiopharmaceutical Dosimetry Symposium, Shalafke-Stelson AT, Watson EE (eds), pp. 346-358, Springfield, VA., NTIS, CONF-85113, 1985.

27. Kearfott KJ. Radiation absorbed dose estimates for positron emission tomography (PET): K-38, Rb-81, Rb-82, and Cs-130. J Nucl Med 23:1128-1132, 1982.

28. International Commission on Radiological Protection. Limits for intakes by workers. ICRP Publication 30, Part 2. Pergamon Press, Oxford, 1980.

29. Cristy M, Eckerman KF. SEECAL: Program to calculate age-dependent specific effective energies. ORNL/TM-12351, Oak Ridge National Laboratory, Oak Ridge, TN, 1993.